

Testing the $E_{p,i}$ - $L_{p,iso}$ - $T_{0.45}$ correlation on a *BeppoSAX* and *Swift* sample of gamma-ray bursts

F. Rossi ¹, C. Guidorzi ^{2,3}, L. Amati ⁴, F. Frontera ^{1,4}, P. Romano ^{2,3}, S. Campana ³, G. Chincarini ^{2,3}, E. Montanari ^{1,5}, A. Moretti ³, G. Tagliaferri ³

¹Dipartimento di Fisica, Università di Ferrara, via Saragat 1, I-44100 Ferrara, Italy

²Dipartimento di Fisica, Università di Milano Bicocca, Piazza delle Scienze 3, I-20126, Milano, Italy

³INAF, Osservatorio Astronomico di Brera, via Bianchi, 46, I-23807 Merate (LC), Italy

⁴Istituto Astrofisica Spaziale e Fisica Cosmica, section of Bologna, CNR/INAF, Via Gobetti 101, I-40129 Bologna, Italy

⁵I. I. S. “I. Calvi”, Finale Emilia (MO), Italy

ABSTRACT

Using a sample of 14 *BeppoSAX* and 74 *Swift* GRBs with measured redshift we tested the correlation between the intrinsic peak energy of the time-integrated spectrum, $E_{p,i}$, the isotropic-equivalent peak luminosity, $L_{p,iso}$, and the duration of the most intense parts of the GRB computed as $T_{0.45}$ (“Firmani correlation”). For 41 out of 88 GRBs we could estimate all of the three required properties. Apart from 980425, which appears to be a definite outlier and notoriously peculiar in many respects, we used 40 GRBs to fit the correlation with the maximum likelihood method discussed by D’Agostini, suitable to account for the extrinsic scatter in addition to the intrinsic uncertainties affecting every single GRB. We confirm the correlation. However, unlike the results by Firmani et al., we found that the correlation does have a logarithmic scatter comparable with that of the $E_{p,i}$ - E_{iso} (“Amati”) correlation. We also find that the slope of the product $L_{p,iso} T_{0.45}$ is equal to -0.5 , which is consistent with the hypothesis that the $E_{p,i}$ - $L_{p,iso}$ - $T_{0.45}$ correlation is equivalent to the $E_{p,i}$ - E_{iso} correlation (slope -0.5). We conclude that, based on presently available data, there is no clear evidence that the $E_{p,i}$ - $L_{p,iso}$ - $T_{0.45}$ correlation is different (both in terms of slope and dispersion) from the $E_{p,i}$ - E_{iso} correlation.

Key words: gamma-rays: bursts – methods: data analysis

1 INTRODUCTION

Ten years after the first measurements of the cosmological distances to Gamma-Ray Bursts (GRBs) made possible by the *BeppoSAX* satellite (Boella et al. 1997), the task of measuring the redshift either of their afterglow itself or of the host galaxy associated with a GRB remains challenging. In the era of the *Swift* spacecraft (Gehrels et al. 2004) the rate of GRBs with a measured distance has increased remarkably thanks to its rapid follow-up capabilities and its arcsec X-ray localisations promptly distributed for most GRBs. Yet, only for one third out of over 300 GRBs detected to date (April 2008) the redshift measurement is available. In the remaining cases, due to the combination of unfavourable observing conditions, such as high Galactic extinction or intrinsic faintness of the afterglow or unavailability of equipped telescopes especially with the NIR filters for high- z GRBs, the attempt is doomed to failure (e.g., see Fynbo et al., 2007).

With respect to the long duration GRBs with known redshift, several correlations between intrinsic properties have already been discovered (e.g. see Schaefer & Collazzi 2007). The interest in these correlations is twofold: they are a direct way to test the pre-

dictions of the emission mechanisms models and, in perspective, they could potentially be used as luminosity estimators. Among the most popular and debated examples, we mention the relation discovered by Amati et al. (2002) between the rest-frame peak energy of the high-energy F spectrum of the prompt emission, $E_{p,i}$, and the isotropic-equivalent radiated energy in the rest-frame 1–10000 keV energy band, E_{iso} , that shows a dispersion of the data points with $\log E_{p,i} = 0.15 \pm 0.04$ (Amati 2006). A tighter correlation has been found afterwards between $E_{p,i}$ and the collimation-corrected radiated energy, E_{γ} , where the jet angle is derived from the time of the break in the afterglow light curve (Ghirlanda et al. 2004). Both relations are still a matter of debate. Criticisms to the $E_{p,i}$ - E_{iso} relation have been raised by Nakar & Piran (2005) and Band & Preece (2005), who claim that the majority of GRBs with unknown redshift detected with *CGRO/BATSE* (Paciesas et al. 1999) are inconsistent with this relation. However, different results have been reported by other authors (Ghirlanda et al. 2005b; Pizzichini et al. 2006). See Amati (2006) for an updated review on this subject. In the case of the $E_{p,i}$ - E_{γ} , what appears to be a crucial and often controversial task is the identification of the break

(if any) in the afterglow light curve due to the jet (Panaitescu et al. 2006; Ghirlanda et al. 2007; Campana et al. 2007). A similar and less model-dependent relation has been found between $E_{p;i}$, E_{iso} and the rest-frame break time of the optical afterglow light curve t_b (Liang & Zhang 2005).

Other correlations have been reported in the literature, such as that between the temporal variability of the time profile and the peak luminosity (Fenimore & Ramirez-Ruiz 2000; Reichart et al. 2001; Schaefer et al. 2001). However, recent work based on larger samples proved that the dispersion of this relation is so large as to make it a useless luminosity estimator (Guidorzi et al. 2005; Guidorzi 2005; Rizzuto et al. 2007).

The correlation found by Norris et al. (2000) between peak luminosity and spectral lag (estimated by cross-correlating time profiles of the same GRB at different energy bands) appears to be a promising tool for identifying the short duration GRBs characterised by an initial spike, followed by a soft and long tail, which otherwise may look like long GRBs (Norris & Bonnell 2006).

In this paper we focus on the correlation discovered by Firmani et al. (2006) involving three properties of the GRB prompt emission: $E_{p;i}$, the isotropic-equivalent peak luminosity in the rest-frame 1–10000 keV band, $L_{p;iso}$, and the smoothing timescale $T_{0:45}$ as defined by Reichart et al. (2001). This correlation ($L_{p;iso} / E_{p;i}^{1:62} T_{0:45}^{0:49}$) was derived from a sample of 22 GRBs and was found to be very tight. This feature would make it an ideal luminosity estimator. In fact, if one assumes $E_{iso} / L_{p;iso} T_{0:45}$ and the validity of the $E_{p;i}$ - E_{iso} relation, the above correlation follows straightforwardly.

We test the $E_{p;i}$ - $L_{p;iso}$ - $T_{0:45}$ correlation using a larger sample (88) of GRBs with known redshift from *BeppoSAX* and *Swift*. In particular, we study $E_{p;i}$ as a function of $L_{p;iso}$ and $T_{0:45}$ to compare its dispersion with that of the $E_{p;i}$ - E_{iso} relation. In Section 2 we present our sample of GRBs; in Section 3 we illustrate the data analysis. In Section 4 we present and discuss our results.

2 THE GRB SAMPLE

The sample of 88 long GRBs with known redshift includes 14 GRBs detected by the Gamma-Ray Burst Monitor (GRBM; Feroci et al., 1997; Frontera et al., 1997; Costa et al., 1998) aboard *BeppoSAX* and 74 by the Burst Alert Telescope (BAT; Barthelmy, 2005) aboard *Swift*. For the latter we consider the GRBs from January 2005 to April 2008. Table 1 reports the full list of GRBs of our sample.

The shortest time binning available for the *BeppoSAX*/GRBM data was 7.8125 ms in the 40–700 keV energy band. For the *Swift*/BAT data the time binning was set to 64 ms in order to ensure a good signal-to-noise (SNR) ratio.

For the GRBM data we considered all the GRBs with known redshift that have a firm estimate of $E_{p;i}$ as reported in Amati (2006) and for which high resolution data were acquired (because of this, we excluded 980613, 011211). For 990510 we used the BATSE data with 64 ms time binning. For 000210 we considered the light curve as in Guidorzi et al. (2005).

As far as BAT GRBs are regarded, we selected only the events whose -ray profile is entirely covered by BAT during the burst mode. Due to these selection criteria we rejected 050318, 050820A, 050904, 060218 and 060906. GRB 060124 was not included in the sample because only the precursor was recorded in burst mode (Romano et al. 2006), while the main event was covered by the sur-

vey mode, whose coarse time resolution makes it unsuitable to our aim.

3 DATA ANALYSIS

3.1 $T_{0:45}$

The smoothing timescale T_f , defined by Reichart et al. (2001) for the calculation of the variability, is the shortest cumulative time interval covering the 100% of the total counts above the background. The fraction f was set to 0.45 because it was originally found to maximise the correlation between variability and peak luminosity (Reichart et al. 2001). A correct evaluation of $T_{0:45}$ must fulfil the requirements found by Guidorzi et al. (2005). For the BAT and GRBM GRBs already published, the values of $T_{0:45}$ are consistent with those reported by Rizzuto et al. (2007) and Guidorzi et al. (2005), respectively. The $T_{0:45}$ of GRB 980703 reported in this paper differs from that reported by Guidorzi et al. (2005) and is consistent with that obtained by Reichart et al. (2001) on BATSE data. However, we verified that this had a negligible impact on the variability estimate obtained by Guidorzi et al. (2005) for this specific GRB.

3.1.1 $T_{0:45}$ as function of energy

In our sample we have two data sets, one for GRBM events in the 40–700 keV band, the other for BAT events in the 15–150 keV band. Given that the value of $T_{0:45}$ is dependent on the energy band used, we modelled this dependence with a power law, similarly to what originally done by Fenimore et al. (1995), for the energy dependence of the autocorrelation function width.

We considered 284 *Swift*/BAT GRBs (all the *Swift*/BAT GRBs from January 2005 to April 2008 regardless of the redshift availability) and for each of them we calculated $T_{0:45}$ in the four nominal BAT energy channels: 15–25, 25–50, 50–100 and 100–150 keV. We focused on the GRBs with an accurate value of $T_{0:45}$ in, at least, three BAT energy channels. As a consequence, only 164 GRBs were selected. For each of them we modelled $T_{0:45}$ with a power law: $T_{0:45}(E) \propto E^{\alpha}$. Figure 1 shows the distribution of the power-law index α : this is consistent with being normally distributed around the mean value of 0.23 and $\sigma = 0.15$. We note that this dependence on energy is marginally less strong than that obtained for the autocorrelation function width by Fenimore et al. (2005; power-law index of 0.4) with BATSE and fully consistent with the energy dependence of the autocorrelation function width found by Borgonovo et al. (2007) for a sample of 19 *BeppoSAX* GRBs. This is not surprising, given that the BAT energy band (15–150 keV) is somewhat between that of the *BeppoSAX*/WFC+GRBM (2–700 keV) and that of BATSE (> 25 keV).

In order to establish the best reference energy E_r at which we have to estimate $T_{0:45}$ in the rest frame (obtained dividing the observed $T_{0:45,obs}$ by $(1+z)$), for all GRBs in our sample we adopted the following approach. Given that $T_{0:45,obs}$ of each GRB is mostly dominated by photons with energies close to their mean energy, for each GRB i in our sample we first determined its rest-frame mean energy $E_{m,i}$. The best rest-frame energy E_r was obtained by performing a logarithmic mean of the derived $E_{m,i}$, finding for the entire sample a value $E_r = 145$ keV. The values of $T_{0:45}$ at this energy are reported in Table 1.

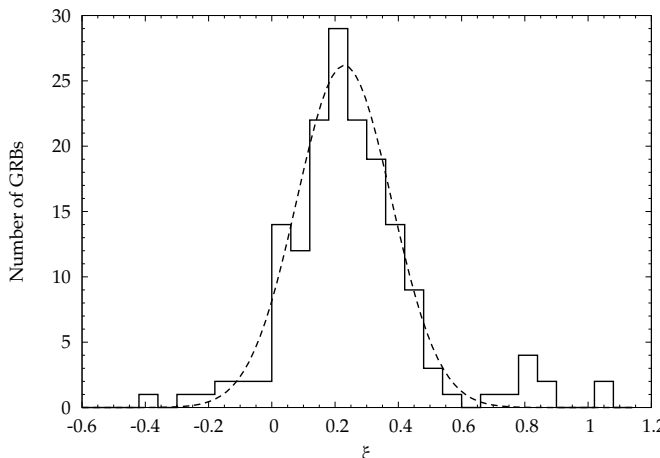


Figure 1. Distribution of the power-law index ξ modelling the dependence of $T_{0:45}$ on energy. The dashed line shows the best-fitting normal distribution centred on $\bar{\xi} = 0.23$ and $\sigma = 0.15$.

3.2 $E_{p,i}$

For each GRB in our sample we evaluated the rest-frame peak energy $E_{p,i}$ of the E (E) time averaged spectrum. For the *BeppoSAX* GRBs we considered the approach followed by Amati et al. (2002), i.e., we fitted the spectra with a smoothly joined power-law proposed by Band et al. (1993), whose parameters, in addition to the normalisation, are the break energy E_0 , and the low and high energy indices α and β , respectively.

For the *Swift/BAT* GRBs, to obtain a firm estimate of $E_{p,i}$ the above approach was not always possible because of the relatively narrow BAT energy band. Therefore, when available, we adopted the $E_{p,i}$ values obtained for the same GRBs with the *Konus/WIND* experiment. In the other cases, we used the values derived from the BAT spectra averaged over the T_{90} interval. The estimated values or their upper/lower limits are generally quite consistent with those reported by Butler et al. (2007) and Sakamoto et al. (2007).

We also checked other integration times of the BAT spectra, e.g., time intervals based on a significance threshold with respect to the background for each GRB, finding photon indices slightly softer than those reported in Table 2, but the statistical quality of the spectra was worse.

3.3 $L_{p,iso}$

The GRB peak luminosity, $L_{p,iso}$, in the source cosmological rest-frame 1–10000 keV energy band is given by:

$$L_{p,iso} = 4 \pi D_L^2(z) \int_{E_p}^{10000/(1+z)} E \langle E \rangle dE \quad (1)$$

where $\langle E \rangle$ is the measured spectrum at the peak ($\text{ph cm}^{-2} \text{s}^{-1} \text{keV}^{-1}$), D_L is the luminosity distance at redshift z (using $H_0 = 71 \text{ km s}^{-1} \text{Mpc}^{-1}$, $\Omega_m = 0.27$ and $\Omega_\Lambda = 0.73$) and E is the energy expressed in keV.

Depending on the morphology of the main pulse (e.g. smooth or spiky), the peak flux, and thus $L_{p,iso}$, may vary up to a factor 1.5–2 when different time scales are considered for its computation (e.g., from the commonly used 1 s to 64 ms time scale). It must also be noted that a fixed time scale in the observed light

curve corresponds to different rest-frame time scales for GRBs at different redshifts, thus providing peak luminosities computed in an inhomogeneous way. In addition, the spectral shape at the peak is often uncertain, because of the low statistical quality of the data and/or the limited number of channels and integration times for time resolved spectra provided by instruments. This is particularly true for *Swift/BAT*, because of its narrow energy band, and for *BeppoSAX/GRBM*, which provided time resolved spectra only in 2 channels and with a time resolution of 1 s.

We computed the peak luminosities of the GRBs included in our sample by following three different methods. First of all, in order to perform a comparison between our and their results, we followed the same method used by Firmani et al. (2006). We extracted the peak spectrum integrated over 1 s and fit it with a Band model in which α , β and E_0 were frozen to the best-fitting values obtained for the spectrum averaged on the entire GRB time profile, while the normalisation was left free to vary. This method is the most commonly used in the literature, e.g., in works studying the $L_{p,iso}$ - $E_{p,i}$ correlation (Ghirlanda et al. 2005a; Yonetoku et al. 2004). We call this “1 s” time scale method.

In the second case, we computed $L_{p,iso}$ using for each GRB the spectrum integrated over the shortest time interval around its peak so as to have a significant number of counts for each energy channel. The spectrum was then fit by still freezing α , β and E_0 to the corresponding values of the time-averaged spectrum, as done for the previous method. We call this “variable” time scale method.

We also attempted to evaluate $L_{p,iso}$ by fitting the spectrum integrated over the variable time scale, as above, with all the spectral parameters left free to vary. In principle this should be the best method for the peak luminosity estimate. However, the statistical quality of these spectra, their narrow energy passband (in the case of BAT), the low number of channel spectra above 30 keV (in the case of GRBM) did not allow to get well constrained estimates of the GRB peak luminosity.

In the following text, in the Tables and in the Figures we call the peak luminosities computed with the two different methods described above as $L_{p,1s}$ and $L_{p,var}$, respectively. The results of both methods are reported in Table 1.

4 RESULTS

In order to study the dependence of $E_{p,i}$ on both $L_{p,iso}$ and $T_{0:45}$, we first used the 40 GRBs in our sample (see Table 1) for which we have a firm determination of $E_{p,i}$, $L_{p,iso}$ and $T_{0:45}$. We applied the maximum likelihood method (hereafter MLM) discussed by D’Agostini (2005) extended to three variables. This method, already adopted by us for other correlation studies (see Guidorzi et al. 2006; Amati 2006), is the best tool to take into account, in addition to the statistical uncertainty in the parameters, the so called extrinsic (or external) scatter, that is the scatter due to the presence of unknown variables that influence the correlation to be tested.

We modelled the correlation among $E_{p,i}$, $L_{p,iso}$ and $T_{0:45}$, according to the equation

$$\log(E_{p,i}) = a \log(L_{p,iso}) + b \log(T_{0:45}) + q \quad (2)$$

where the four parameters a , b , q and the extrinsic scatter $\log E_{p,i}$ are free to vary in the fit. The best-fitting parameters so obtained, for each of the two peak luminosity estimates, are reported in Table 2, together with their uncertainties (at 90% confidence level), and the best fit χ^2 and chance probability.

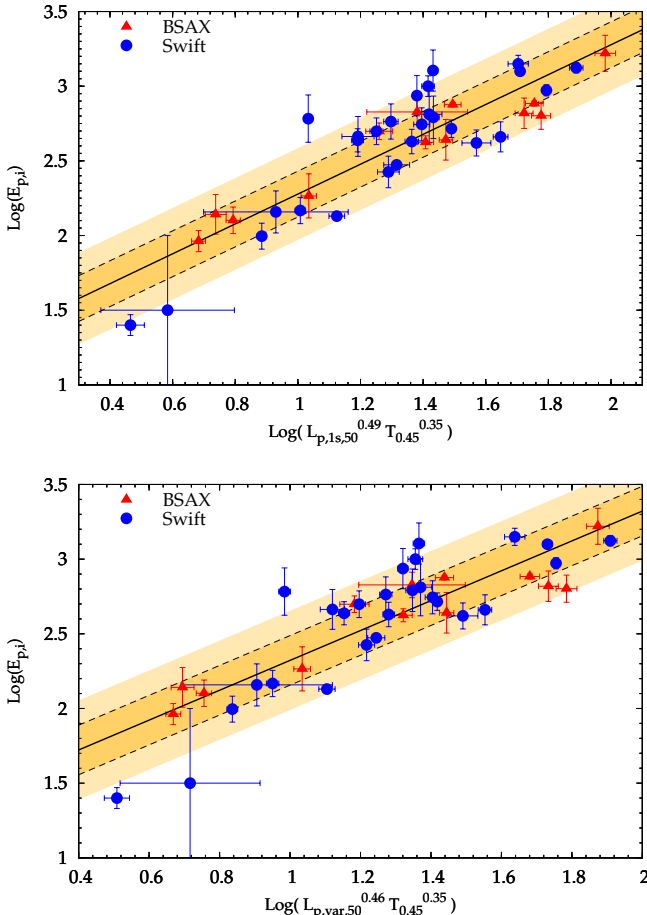


Figure 2. Peak energy $E_{p;i}$ as a function of $L_{p;iso}$ and $T_{0:45}$. Only GRBs with firm estimates of all of the properties are shown. Triangles (circles) correspond to *BeppeSAX* (*Swift*) GRBs. Peak luminosities are expressed in units of 10^{50} erg s $^{-1}$. In the top plot the peak luminosity used is $L_{p;1s}$, in the bottom it is $L_{p;var}$ (see text). The solid line shows the best fit curve obtained with the maximum likelihood method illustrated by D'Agostini (2005). Dashed lines represent the 1- and 2- σ regions. ζ is the best-fit value found for $\log E_{p;i}$ in each case.

As can be seen from this Table, for both $L_{p;1s}$ and $L_{p;var}$ estimates of $L_{p;iso}$, we find a significant value of extrinsic scatter, as displayed in Fig. 2. This result is confirmed by the fit of the data with Eq. 2, freezing $\log E_{p;i}$ to 0. The resulting fit, also reported in Table 2, is highly unacceptable.

GRB 980425 was found not to follow at all the correlation, as in the case of the other relations, such as the $E_{p;i}$ - E_{iso} (Amati et al. 2002), the lag-luminosity (Norris et al. 2000) and the variability-luminosity (Reichart et al. 2001) ones. This GRB is also peculiar for several aspects, such as its being subluminous and its association with SN1998bw, thanks to which it was possible to measure its relatively close (~40 Mpc) distance. Therefore, like Firmani et al. (2006), we did not include it in the sample used to derive the fit results in Table 2, and we focused on the canonical long-duration GRBs and XRFs which are known to follow all of the main correlations. If we include GRB 980425 in the sample, its contribution to the dispersion of the correlation is remarkable: in the $L_{p;1s}$ case, the extrinsic scatter passes from $0.15^{+0.05}_{-0.03}$ to 0.22 ± 0.05 (the

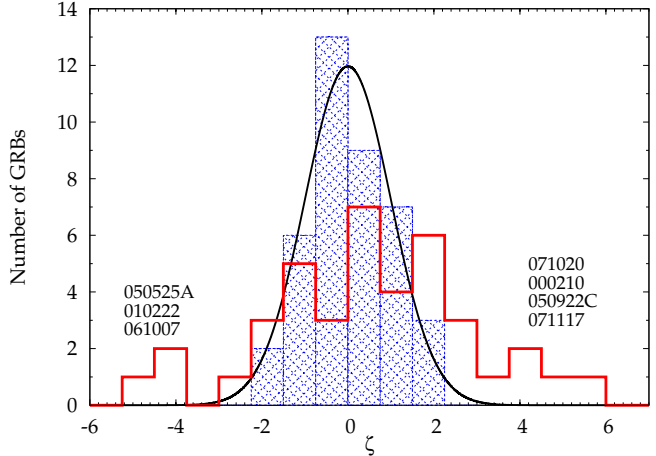


Figure 4. The shaded (thick line) histogram shows the distribution of the normalised scatter (not) inclusive of the extrinsic scatter. The expected normal $N(0;1)$ is also displayed. The peak luminosity used is $L_{p;1s}$.

other parameters becoming $a = 0.32 \pm 0.06$, $b = 0.29 \pm 0.16$ and $q = 1.73 \pm 0.19$, respectively). Similar results are obtained using $L_{p;var}$.

Moreover, we applied the MLM also to the subsample of 27 *Swift* GRBs with determined $E_{p;i}$, $T_{0:45}$ and $L_{p;iso}$. The results, reported in Table 2, clearly show that also in this case the extrinsic scatter, $\log E_{p;i} = 0.17 \pm 0.04$ ($L_{p;1s}$), is fully consistent with that derived from the entire sample and far from being negligible. This proves that the extrinsic scatter is a property of the correlation itself and not an artifact of merging data sets from different instruments.

Including all GRBs in our sample, the data points are shown in Fig. 3, where we report also the best fit relation between $E_{p;i}$, L_p and $T_{0:45}$ in the case of the $L_{p;1s}$ estimate and with the extrinsic scatter taken into account. As can be seen from this figure, in addition to many lower or upper limits to $E_{p;i}$ potentially consistent with the correlation, a few of them clearly deviate by more than 2 from the best fit model.

In order to understand the origin the extrinsic scatter, we studied the distribution $N(\zeta)$ of the normalised deviation of the measured $\log E_{p;i}$ from the values expected on the basis of the best fit curve (Eq. 2) in two cases, i.e., by including or excluding the found extrinsic scatter $\log E_{p;i}$:

$$\zeta_i = \frac{(a \log L_{p;iso}^{(i)} + b \log T_{0:45}^{(i)} + q) - \log E_{p;i}^{(i)}}{\sqrt{\frac{1}{2} \left(\frac{a^2}{\log E_{p;i}^{(i)}} + \frac{b^2}{\log L_{p;iso}^{(i)}} + \frac{2}{\log T_{0:45}^{(i)}} \right) + \frac{2}{\log E_{p;i}^{(i)}}}} \quad (3)$$

Figure 4 shows the result in the case of the peak luminosity estimate $L_{p;1s}$. When the extrinsic scatter is taken into account, the resulting distribution (shaded histogram) is consistent with a normalised Gaussian, consistently with the picture of an extrinsic scatter characterising the correlation itself. Instead, assuming no extrinsic scatter ($\log E_{p;i} = 0$), we find an histogram (see the thick line in Fig. 4) clearly inconsistent with the normalised Gaussian. In addition to seven apparent outliers lying $> 3 \sigma$ off (071020, $+5.5^\circ$; 000210, $+4.4^\circ$; 071117, $+3.9^\circ$; 050922C, $+3.8^\circ$; 050525A, $+2.2^\circ$; 061007, $+4.0^\circ$; 010222, $+4.0^\circ$), others GRBs contribute to broaden the histogram, making it inconsistent with a normalised Gaussian.

We have carefully checked the adopted estimates of $E_{p;i}$,

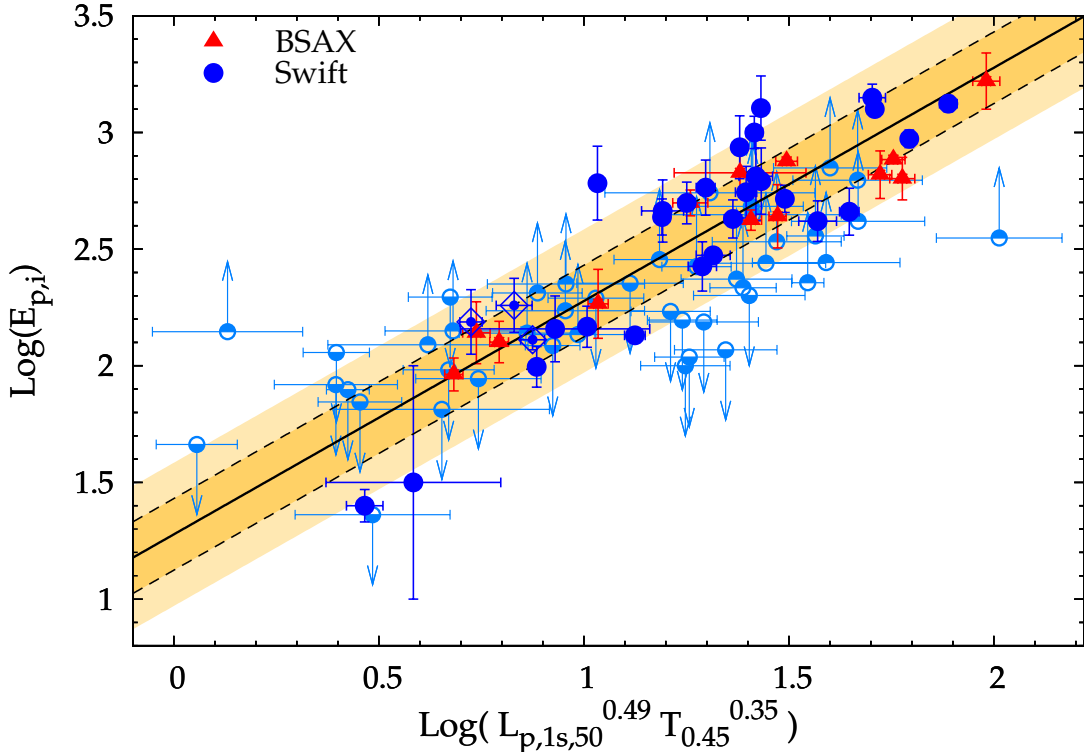


Figure 3. Peak energy $E_{p,i}$ as a function of $L_{p,1s}$ and $T_{0,45}$ using all GRBs in our sample. Triangles (circles) correspond to *BeppoSAX* (*Swift*) GRBs. Dashed lines represent the 1- σ region. Shaded areas show the 1- and 2- σ regions. α is the best-fit value found for $\log E_{p,i}$. The empty diamonds show the three *Swift* GRBs, 070506, 070611 and 070810A, for which we constrained $E_{p,i}$ but which were not used to fit correlation (see text).

$L_{p,iso}$ and $T_{0,45}$ attributed to the outliers, finding that they are robust. For example, in the case of GRB 000210 (a *BeppoSAX* GRB) we confirm the correctness of the attributed values. In the case of GRB 050525A, the accurate estimate of $E_{p,i}$ was provided by the *Konus/WIND* experiment and we see no reason to reject it.

Similar results are obtained when the same analysis is performed using $L_{p,var}$ as peak luminosity estimate.

5 DISCUSSION

After the discovery by Firmani et al. (2006) of a correlation among the rest frame quantities $E_{p,i}$, $L_{p,iso}$, and $T_{0,45}$, obtained with a sample of 22 GRBs ('Firmani' relation), using a larger GRB sample (88 GRBs with known redshift detected by *BeppoSAX* and *Swift*) the correlation has been re-tested. By ignoring the outlier GRB 980425 and 47 GRBs for which only upper/lower limits to $E_{p,i}$ were possible to be established, we confirm the correlation with only slightly different best-fitting parameters (see Table 2). However, unlike Firmani et al. (2006) we find a significant extrinsic dispersion of the data points around the best fit curve, parametrised by the $\log E_{p,i}$ value reported in Table 2, that denotes the presence of an unknown variable (see D'Agostini 2005). This scatter is found to be independent of the time integration of the measured spectra (either 1 s for all GRBs or variable from a GRB to another depending on the light curve shape and statistical quality) used to estimate of $L_{p,iso}$.

It is also apparent from the χ^2/dof reported Table 2, that as-

suming a null extrinsic scatter gives unacceptable results. We have analysed the origin of the extrinsic scatter and found that, in addition to seven clear outliers, other GRBs contribute to the found dispersion. From a detailed analysis of the data available for each of the 40 GRB included in our reduced sample, we cannot find any reason to infer that some of the estimates reported in Table 2 is unreliable.

Furthermore, as can be seen in Fig. 3, also some GRBs with only upper/lower limits deviate form the best fit curve by more than 2σ . Thus, the distribution of GRBs in the correlation plane found by us is not as tight as that found by Firmani et al. (2006) using a smaller sample of 22 events.

On the basis of the reported results, we derive an interesting consequence. Taking into account that, in the $E_{p,i}$, $L_{p,iso}$, $T_{0,45}$ multivariate correlation, the best-fitting power-law indices for $L_{p,iso}$ and $T_{0,45}$ (see Table 2) are both consistent with 0.5, we infer that the Firmani relation can be approximately written as

$$E_{p,i} / (L_{p,1s} T_{0,45})^{0.5} \quad (4)$$

That renders the Firmani relation equivalent to the $E_{p,i}$ vs. E_{iso} relation discovered by Amati et al. (2002). Also the obtained extrinsic scatter is consistent with that of the Amati relation (Amati 2006). In conclusion, it seems that the Firmani relation does not provide more information than that contained in the Amati relation. It is expected that the future joint observations by *Swift* and *GLAST* will provide a sizable set of GRBs with firm measures of all the required observables, thus allowing to refine the estimate of

the dispersion and to better characterise its link with the $E_p;_i-E_{iso}$ relation.

Table 1. The GRB sample: $T_{f=0:45}$ (at the rest-frame energy of $E_r = 145$ keV), the intrinsic peak energy, $E_{p,i}$, and the peak luminosities $L_{p,ls}$ and $L_{p,var}$.

GRB Name	z Redshift	Inst. ^(a) 2	$T_{f=0:45}$ (s) 3	$E_{p,i}$ (keV) 4	$t_{start,ls}^{(b)}$ (s) 5	$L_{p,ls}^{(c)}$ (10^{50} erg s $^{-1}$) 6	$t_{start,var}^{(b)}$ (s) 8	$t_{stop,var}^{(b)}$ (s) 9	$L_{p,var}^{(c)}$ (10^{50} erg s $^{-1}$) 10	z Reference ^d 11	$E_{p,i}$ Reference ^e 12					
970228 ^f	0.695	G	$1.54^{+0.18}_{-0.19}$	195	64	0:437	95	7	0:680	0:774	130	10	1	1		
970508 ^f	0.835	G	$1.70^{+0.31}_{-0.29}$	145	43	0:133	22	2	0:196	1:132	22	2	2	1		
971214 ^f	3.42	G	$1.45^{+0.39}_{-0.31}$	680	130	10:857	650	400	6:068	6:248	830	520	3	1		
980425	0.0085	G	$4.46^{+0.25}_{-0.25}$	55	21	3:977	(6:6	0:6)	10 ⁴	2:797	4:945	(6:0	0:6)	10 ⁴	4	1
980703 ^f	0.966	G	$11.52^{+2.68}_{-2.50}$	503	64	2:656	65	8	2:456	4:456	60	7	5	1		
990123 ^f	1.60	G	$6.54^{+1.39}_{-1.34}$	1720	470	6:758	2850	200	6:750	7:172	2900	200	6	1		
990506 ^f	1.30	G	$4.84^{+0.50}_{-0.46}$	680	160	87:055	1050	60	90:180	90:202	1800	100	7	1		
990510 ^f	1.619	G	$1.53^{+0.24}_{-0.22}$	423	42	40:332	550	30	40:332	41:332	550	30	8	1		
990705 ^f	0.86	G	$7.94^{+1.08}_{-0.95}$	460	140	10:514	230	10	20:842	20:936	290	10	9, 10	1		
990712 ^f	0.434	G	$3.54^{+0.26}_{-0.25}$	93	15	0:625	10	1	0:679	1:046	11	1	11	1		
991216 ^f	1.02	G	$1.67^{+0.24}_{-0.24}$	650	130	3:289	2900	220	4:156	4:172	5200	400	12	1		
000210 ^f	0.846	G	$1.06^{+0.16}_{-0.14}$	750	30	3:022	1100	80	3:248	3:310	1300	100	13	1		
010222 ^f	1.477	G	$3.42^{+0.62}_{-0.53}$	766	30	58:680	1600	90	58:875	58:953	1800	100	14	2		
010921 ^f	0.45	G	$5.04^{+0.53}_{-0.51}$	129	26	10:383	13	1	9:586	10:930	13	1	15	1		
050126	1.29	B	$5.00^{+0.67}_{-0.52}$	>	172	4:112	-	-	2:448	5:008	-	-	16	3		
050223	0.5915	B	$4.98^{+0.88}_{-1.00}$	<	114	1:584	-	-	6:256	11:120	-	-	17	3		
050315	1.949	B	$6.19^{+0.42}_{-0.41}$	<	109	24:592	-	-	24:720	25:296	-	-	18	3		
050319	3.240	B	$3.38^{+0.31}_{-0.46}$	<	157	0:656	-	-	0:336	0:976	-	-	19	3		
050401 ^f	2.90	B	$1.43^{+0.13}_{-0.12}$	470	110	24:248	1780	160	24:760	25:272	1850	130	20	1		
050416A ^f	0.6535	B	$0.70^{+0.15}_{-0.14}$	$25.1^{+4.4}_{-3.7}$	0:064	11:7	1:7	-	0:704	0:896	17:0	1:4	21	1		
050505	4.27	B	$2.72^{+0.31}_{-0.43}$	>	416	1:000	-	-	1:000	2:024	-	-	22	3		
050525A ^f	0.606	B	$1.37^{+0.17}_{-0.15}$	135	3	0:848	157	13	1:232	1:360	200	15	23	1		
050603 ^f	2.821	B	$0.68^{+0.06}_{-0.06}$	1330	110	0:184	9400	700	0:136	0:264	19300	1200	24	1		
050730	3.967	B	$12.06^{+1.12}_{-1.10}$	>	705	4:408	-	-	2:488	7:288	-	-	25	3		
050803	0.422	B	$11.94^{+1.72}_{-1.77}$	>	123	147:208	-	-	147:528	147:848	-	-	26	3		
050814	5.30	B	$7.44^{+1.25}_{-1.21}$	>	227	8:712	-	-	3:976	13:256	-	-	27	3		
050824	0.83	B	$4.55^{+1.28}_{-1.20}$	<	23	53:128	-	-	47:816	54:280	-	-	28	3		
050826	0.297	B	$6.95^{+1.38}_{-1.32}$	>	140	1:328	-	-	0:208	2:608	-	-	29	3		
050908	3.3437	B	$1.68^{+0.21}_{-0.22}$	<	226	2:080	-	-	1:760	3:104	-	-	30	3		
050922C ^f	2.198	B	$0.43^{+0.02}_{-0.04}$	417^{+102}_{-54}	0:072	510	40	0:696	0:824	640	40	19	1			
051016B	0.936	B	$1.41^{+0.30}_{-0.23}$	<	70	0:072	-	-	0:456	0:840	-	-	31	3		
051109A ^f	2.346	B	$3.16^{+0.60}_{-0.40}$	540^{+470}_{-120}	0:424	340	50	0:872	1:448	400	44	32	1			
051111	1.55	B	$4.21^{+0.17}_{-0.27}$	>	275	0:304	-	-	0:304	0:016	-	-	33	3		
060115 ^f	3.53	B	$6.32^{+0.487}_{-0.487}$	272^{+68}_{-63}	94:896	110	20	94:640	96:240	111	11	34	3			
060206 ^f	4.048	B	$0.83^{+0.07}_{-0.07}$	394^{+120}_{-41}	2:168	700	60	2:680	3:192	710	40	35	3			
060210	3.91	B	$9.19^{+0.84}_{-0.81}$	>	353	0:040	-	-	0:216	0:472	-	-	36	3		
060223A	4.41	B	$1.36^{+0.20}_{-0.20}$	>	216	0:072	-	-	0:248	0:456	-	-	37	3		
060418 ^f	1.489	B	$6.27^{+0.38}_{-0.37}$	570	140	27:472	190	20	27:600	27:664	285	30	38	4		
060502A	1.51	B	$3.52^{+0.27}_{-0.27}$	>	444	0:112	-	-	0:848	1:520	-	-	39	3		
060510B	4.90	B	$17.32^{+1.43}_{-1.61}$	>	360	136:360	-	-	133:032	138:920	-	-	40	3		

Table 1 (cont'd)

GRB Name	z Redshift	Inst. ^(a)	T _{f=0:45} (s)	E _{p,i} (keV)	t _{start;ls} (s)	L _{p;ls} (10 ⁵⁰ erg s ⁻¹)	t _{start;var} (s)	t _{stop;var} (s)	L _{p,var} (10 ⁵⁰ erg s ⁻¹)	z	E _{p,i}
1	2	3	4	5	6	7	8	9	10	Reference ^d	Reference ^e
060512	0:443	B	1:91 ^{+ 0:45} 0:51	< 46	3:280	-	0:016	2:768	-	41	3
060522	5:11	B	4:23 ^{+ 0:65} 0:63	> 235	4:392	-	2:792	5:416	-	42	3
060526	3:221	B	4:18 ^{+ 0:45} 0:34	< 154	0:128	-	0:704	1:024	-	19	3
060604	2:68	B	2:63 ^{+ 0:55} 0:55	< 195	2:288	-	1:968	3:312	-	43	3
060605 ^f	3:70	B	4:38 ^{+ 0:54} 0:53	450 ^{+ 180} 110	1:680	96 21	1:680	4:752	91 13	44	3
060607A	3:082	B	5:68 ^{+ 0:31} 0:37	> 277	0:552	-	0:808	0:792	-	45	3
060614 ^f	0:125	B	16:62 ^{+ 3:42} 2:84	55 45	1:360	3:1 2:4	2:864	2:928	6:55 4:95	46	5
060707 ^f	3:425	B	4:96 ^{+ 0:45} 0:44	301 ^{+ 16} 22	1:928	155 28	1:992	4:040	154 16	19	3
060714	2:711	B	6:04 ^{+ 0:26} 0:34	< 171	75:344	-	75:664	76:048	-	19	3
060729	0:54	B	14:52 ^{+ 2:22} 2:07	< 79	92:888	-	91:928	93:976	-	47	3
060814 ^f	0:84	B	11:68 1:09	470 ^{+ 40} 70	15:368	60:9 4:3	15:560	15:880	62:5 3:5	48	6
060904B ^f	0:703	B	3:42 ^{+ 0:48} 0:52	135 ^{+ 64} 31	1:104	54 43	1:680	2:128	61 48	49	3
060908 ^f	2:43	B	1:75 ^{+ 0:08} 0:13	545 ^{+ 220} 100	0:992	300 30	1:184	1:440	390 30	50	3
060912A	0:937	B	0:59 ^{+ 0:08} 0:05	> 205	0:032	-	0:352	0:608	-	51	3
060926	3:208	B	0:73 0:09	< 122	0:352	-	0:480	0:928	-	52	3
060927 ^f	5:60	B	0:67 0:08	400 ^{+ 110} 60	0:168	2170 430	0:808	1:192	2440 470	53	3
061007 ^f	1:262	B	7:38 ^{+ 0:24} 0:26	900 ^{+ 120} 40	45:176	1080 40	38:456	38:520	1460 30	54	7
061110A	0:757	B	8:29 ^{+ 1:34} 1:03	> 141	9:720	-	0:968	3:128	-	55	3
061110B	3:44	B	5:34 ^{+ 0:56} 0:74	> 551	7:872	-	16:128	15:424	-	56	3
061121 ^f	1:314	B	2:21 ^{+ 0:12} 0:11	1400 ^{+ 210} 170	74:456	1700 250	74:840	74:904	2040 280	57	3
061126 ^f	1:1588	B	2:75 ^{+ 0:20} 0:30	1337 410	6:552	409 9	6:680	6:936	446 18	58	8
061222B	3:355	B	3:54 ^{+ 0:28} 0:41	< 200	59:048	-	45:672	47:208	-	59	3
070110	2:352	B	6:41 ^{+ 0:47} 0:36	> 285	0:800	-	0:480	1:760	-	60	3
070208	1:165	B	2:79 0:59	< 197	0:312	-	0:248	0:840	-	61	3
070318	0:836	B	5:69 ^{+ 0:60} 0:50	> 224	1:168	-	1:360	2:192	-	62	3
070411	2:954	B	8:82 0:47	> 482	70:176	-	69:856	71:008	-	63	3
070419A	0:97	B	20:86 ^{+ 4:06} 3:23	< 65	1:304	-	18:600	35:368	-	64	3
070506 ^g	2:31	B	0:52 0:08	162 50	6:312	48:5 3:5	6:376	6:824	57 5	65	3
070529	2:5	B	7:39 ^{+ 1:86} 1:26	> 340	2:008	-	2:392	2:904	-	66	3
070611 ^g	2:04	B	1:67 0:33	188 49	2:336	35 5	1:568	3:744	18 2	67	3
070612A	0:617	B	39:38 ^{+ 4:62} 3:69	> 136	9:704	-	6:248	12:520	-	68	3
070721B	3:626	B	5:06 ^{+ 0:68} 0:66	> 624	0:136	-	0:584	2:120	-	69	3
070802	2:45	B	2:27 0:46	> 138	6:120	-	5:672	10:088	-	70	3
070810A ^g	2:17	B	0:93 0:16	130 13	0:136	65 4	0:120	0:760	66 6	71	3
071010A	0:98	B	1:24 ^{+ 0:46} 0:45	< 83	0:992	-	1:056	4:128	-	72	3
071010B ^f	0:947	B	2:14 ^{+ 0:21} 0:20	101 20	1:432	36:8 0:8	1:944	2:456	37:2 1:0	73	9
071020 ^f	2:145	B	0:51 0:06	1010 160	0:336	1265 25	0:240	0:368	1510 60	74	10
071031	2:692	B	10:53 1:27	< 100	2:880	-	2:624	5:248	-	75	3
071117 ^f	1:331	B	0:53 ^{+ 0:03} 0:05	647 226	0:016	206:5 6:5	0:464	0:656	231 13	76	11
071122	1:14	B	8:94 ^{+ 2:15} 2:12	< 96	11:816	-	10:520	13:352	-	77	3

Table 1 (cont'd)

GRB Name	z Redshift	Inst. ^(a) 3	$T_{f=0:45}$ (s) 4	$E_{p,i}$ (keV) 5	$t_{start;ls}^{(b)}$ (s) 6	$L_{p;ls}^{(c)}$ (10^{50} erg s ⁻¹) 7	$t_{start;var}^{(b)}$ (s) 8	$t_{stop;var}^{(b)}$ (s) 9	$L_{p;var}^{(c)}$ (10^{50} erg s ⁻¹) 10	z Reference ^d 11	$E_{p,i}$ Reference ^e 12
080210	2.641	B	$3.21^{+0.59}_{-0.30}$	> 266	4.448	-	7.072	9.184	-	78	3
080310	2.43	B	$11.68^{+1.18}_{-0.48}$	< 117	1.152	-	1.280	2.176	-	79	3
080319B ^f	0.937	B	$8.23^{+0.48}_{-0.45}$	1261 65	16.848	672.5 6.5	12.420	12.436	1190 60	80	12
080319C ^f	1.95	B	$1.78^{+0.07}_{-0.13}$	910 270	0.128	440 20	0.256	0.512	490 30	81	13
080330	1.51	B	$1.92^{+0.44}_{-0.30}$	< 88	0.128	-	0.384	0.832	-	82	3
080411 ^f	1.03	B	$2.58^{+0.21}_{-0.19}$	524 70	40.448	553.5 5.5	40.960	41.088	595 13	83	14
080413A ^f	2.433	B	$1.74^{+0.20}_{-0.20}$	650 210	1.624	564 16	1.688	2.200	570 20	84	3
080413B ^f	1.10	B	$0.50^{+0.06}_{-0.04}$	150 30	0.224	185 5	0.224	0.480	200 10	85	3

^a Instrument: G (GRBM), B(BAT)

^b Times of the spectrum accumulated around the peak. They are given with reference to the GRBM (BAT) trigger time of each *BeppoSAX* (*Swift*) GRB.

^c Peak bolometric isotropic equivalent luminosity in 10^{50} erg s⁻¹ in the rest frame; $H_0 = 71 \text{ km s}^{-1} \text{ Mpc}^{-1}$, $m = 0.27$, and $\Omega = 0.73$.

^d References for the redshift measurements: (1) Djorgovski et al. (1999), (2) Metzger et al. (1997), (3) Kulkarni et al. (1998), (4) Tinney et al. (1998), (5) Djorgovski et al. (1998), (6) Kulkarni et al. (1999), (7) Bloom et al. (2003), (8) Beuermann et al. (1999), (9) Amati et al. (2000), (10) Le Floc'h et al. (2002), (11) Galama et al. (1999), (12) Vreeswijk et al. (1999), (13) Piro et al. (2002), (14) Garnavich et al. (2001), (15) Djorgovski et al. (2001), (16) Berger, Cenko & Kulkarni et al. (2005a), (17) Berger & Shin (2006), (18) Kelson & Berger (2005), (19) Jakobsson et al. (2006a), (20) Fynbo et al. (2005a), (21) Cenko et al. (2005), (22) Berger et al. (2005b), (23) Foley et al. (2005), (24) Berger & Becker (2005), (25) Chen et al. (2005), (26) Bloom et al. (2005), (27) Jakobsson et al. (2006b), (28) Fynbo et al. (2005b), (29) Halpern & Mirabal (2006), (30) Fugazza et al. (2005), (31) Soderberg, Berger & Ofek (2005), (32) Quimby et al. (2005), (33) Hill et al. (2005), (34) Piranomonte et al. (2006), (35) Fynbo et al. (2006a), (36) Cucchiara, Fox & Berger (2006a), (37) Berger et al. (2006a), (38) Dupree et al. (2006), (39) Cucchiara et al. (2006b), (40) Price (2006), (41) Bloom et al. (2006a), (42) Cenko et al. (2006), (43) Castro-Tirado et al. (2006), (44) Still et al. (2006), (45) Ledoux et al. (2006), (46) Fugazza et al. (2006a), (47) Thoene et al. (2006a), (48) Thoene et al. (2007a), (49) Fugazza et al. (2006b), (50) Rol et al. (2006), (51) Levan et al. (2007), (52) D'Elia et al. (2006), (53) Fynbo et al. (2006b), (54) Jakobsson et al. (2006c), (55) Thoene et al. (2006b), (56) Fynbo et al. (2006c), (57) Bloom, Perley & Chen (2006b), (58) Perley et al. (2008), (59) Berger (2006b), (60) Jaunsen et al. (2007a), (61) Cucchiara et al. (2007a), (62) Jaunsen et al. (2007b), (63) Jakobsson et al. (2007a), (64) Cenko et al. (2007a), (65) Thoene et al. (2007b), (66) Berger et al. (2007), (67) Thoene et al. (2007c), (68) Cenko et al. (2007b), (69) Malesani et al. (2007), (70) Prochaska et al. (2007a), (71) Thoene et al. (2007d), (72) Prochaska et al. (2007b), (73) Cenko et al. (2007c), (74) Jakobsson et al. (2007b), (75) Ledoux et al. (2007), (76) Jakobsson et al. (2007c), (77) Cucchiara et al. (2007b), (78) Jakobsson et al. (2008), (79) Prochaska et al. (2008a), (80) Vreeswijk et al. (2008a) (81) Wiersema et al. (2008), (82) Malesani et al. (2008), (83) Thoene et al. (2008a), (84) Thoene et al. (2008b), (85) Vreeswijk et al. (2008b).

^e References for the $E_{p,i}$ measurements: (1) Amati (2006), (2) Ulanov et al. (2005), (3) This work, (4) Golenetskii et al. (2006a) (5) Amati et al. (2007), (6) Golenetskii et al. (2006b), (7) Mundell (2007), (8) Perley et al. (2008), (9) Golenetskii et al. (2007a), (10) Golenetskii et al. (2007b), (11) Golenetskii et al. (2007c), (12) Golenetskii et al. (2008a), (13) Golenetskii et al. (2008b), (14) Golenetskii et al. (2008c).

^f GRBs with firm measurements of $E_{p,i}$, $T_{0:45}$ and $L_{p,iso}$, used to derive the best-fitting parameters of the correlation.

^g From the BAT data we could constrain only $E_{p,i}$, while no information on $T_{0:45}$ and $L_{p,iso}$ could be derived. These values for $E_{p,i}$ are not confirmed by Sakamoto et al. (2007). These GRBs were not included in the sample used to fit the correlation, but just displayed in Fig. 3. Their peak luminosities were computed assuming $T_{0:45} = 1$ and $L_{p,iso} = 2.3$.

ACKNOWLEDGMENTS

We acknowledge the anonymous referee for useful comments. This work is supported by ASI grant I/011/07/0 and by the Ministry of University and Research of Italy (PRIN 2005025417). We gratefully acknowledge the contributions of dozens of members of the BAT team who built and maintain this instrument.

REFERENCES

- Amati L. et al., 2000, *Sci*, 290, 953
 Amati L. et al., 2002, *A&A*, 390, 81
 Amati L., 2006, *MNRAS*, 372, 233
 Amati L. et al., 2007, *A&A*, 463, 913
 Band D. et al., 1993, *ApJ*, 413, 281
 Band D. L., Preece R. D., 2005, *ApJ*, 627, 319
 Barthelmy S. D., et al., 2005, *Space Science Review*, 120, 143
 Berger E., Cenko S. B., Kulkarni S. R., 2005a, *GCN*, 3088
 Berger E., Cenko S. B., Steidel C., Reddy N., Fox D. B., 2005b, *GCN*, 3368
 Berger E., Kulkarni S. R., Rau A., Fox D. B., 2006a, *GCN*, 4815
 Berger E., 2006b, *GCN*, 5962
 Berger E., Becker G., 2005, *GCN*, 3520
 Berger E., Shin M.-S., 2006, *GCN*, 5283
 Berger E., Fox D. B., Cucchiara A., 2007, *GCN*, 6470
 Beuermann K. et al, 1999, *A&A*, 352, L26
 Bloom J. S., Berger E., Kulkarni S. R., Djorgovski S. G., Frail D. A., 2003, *AJ*, 125, 999
 Bloom J. S., Perley D., Foley R., Prochaska J. X., Chen H. W., Starr D., 2005, *GCN*, 3758
 Bloom J. S., Foley R. J., Kocevski D., Perley D., 2006a, *GCN*, 5217
 Bloom J. S., Perley D. A., Chen H. W., 2006b, *GCN*, 5826
 Boella G., Butler R. C., Perola G. C., Piro L., Scarsi L., Bleeker, 1997, *A&AS*, 122, 299
 Borgonovo L., Frontera F., Guidorzi C., Montanari E., Vetere L., Sofitta P., 2007, *A&A*, 465, 765.
 Butler N. R., Locevski D., Bloom J. S., Curtis J. L., 2007, *ApJ*, submitted (astro-ph 0706.1275)
 Campana S., Guidorzi C., Tagliaferri G., Chincarini G., Moretti A., Rizzuto D., Romano P., 2007, *A&A*, 472, 395
 Castro-Tirado A. J., Amado P., Negueruela I., Gorosabel J., Jelinek M., de Ugarte Postigo A., 2006, *GCN*, 5218
 Cenko S. B., Kulkarni S. R., Gal-Yam A., Berger E., 2005, *GCN*, 3542
 Cenko S. B., Berger E., Djorgovski S. G., Mahabal A. A., Fox D. B., 2006, *GCN*, 5155
 Cenko S. B., Gezari S., Small T., Fox D. B., Berger E., 2007a, *GCN*, 6322
 Cenko S. B., Fox D. B., Schmidt B. P., Berger E., Price P. A., Roth K. C., 2007b, *GCN*, 6556
 Cenko S. B., Cucchiara A., Fox D. B., Berger E., Price P. A., 2007c, *GCN*, 6888
 Chen H. W., Thompson I., Prochaska J. X., Bloom J., 2005, *GCN*, 3709
 Costa E. et al., 1998, *Adv.Sp.Res.*, 22, 1129
 Cucchiara A., Fox D. B., Berger E., 2006a, *GCN*, 4729
 Cucchiara A., Price P. A., Fox D. B., Cenko S. B., Schmidt B. P., 2006b, *GCN*, 5052
 Cucchiara A., Fox D. B., Cenko S. B., Price P. A., 2007a, *GCN*, 6083
 Cucchiara A., Fox D. B., Cenko S. B., 2007b, *GCN*, 7124
 D'Agostini G, 2005, *physics/0511182*.
 D'Elia V. et al., 2006, *GCN*, 5637
 Djorgovski S. G., Kulkarni S. R., Bloom J. S., Goodrich R., Frail D. A., Piro L., Palazzi E., 1998, *ApJ*, 508, L17
 Djorgovski S. G., Kulkarni S. R., Bloom J. S., Frail D. A., 1999, *GCN* 289
 Djorgovski S. G. et al., 2001, *GCN* 1108
 Dupree A. K., Falco E., Prochaska J. X., Chen H. W., Bloom J. S., 2006, *GCN*, 4969
 Fenimore E. E., in't Zand J. J. M., Norris J. P., Bonnell J. T., Nemiroff R. J., 1995, *ApJ*, 448, L101
 Fenimore E. E., Ramirez-Ruiz E., 2000, preprint (astro-ph/0004176)
 Feroci M. et al., 1997, *SPIE Conf. Ser.*, 3114, 186
 Firmani C., Ghisellini G., Avila-Reese V., Ghirlanda G., 2006, *MNRAS*, 370, 185
 Foley R. J., Chen H. W., Bloom J. S., Prochaska J. X., 2005, *GCN*, 3483
 Frontera F., Costa E., dal Fiume D., Feroci M., Nicastro L., Orlandini M., Palazzi E., Zavattini G., 1997, *A&AS*, 122, 357
 Fugazza D. et al., 2005, *GCN*, 3948
 Fugazza D. et al., 2006a, *GCN*, 5276
 Fugazza D. et al., 2006b, *GCN*, 5513
 Fynbo J. P. U. et al., 2005a, *GCN*, 3176
 Fynbo J. P. U. et al., 2005b, *GCN*, 3874
 Fynbo J. P. U. et al., 2006a, *A&A*, 451, L47
 Fynbo J. P. U. et al., 2006b, *GCN*, 5651
 Fynbo J. P. U., Malesani D., Thoene C. C., Wreeswijk P. M., Hjorth J., Hemiksen C., 2006c, *GCN*, 5809
 Fynbo J. P. U. et al., 2007, *The ESO Messenger*, 130, 43
 Galama T. J. et al., 1999, *GCN* 388
 Garnavich P. M., Pahre M. A., Jha S., Calkins M., Stanek K. Z., McDowell J., Kilgard R., 2001, *GCN* 965
 Gehrels N. et al., 2004, *ApJ*, 611, 1005
 Ghirlanda G., Ghisellini G., Lazzati D., 2004, *ApJ*, 616, 331
 Ghirlanda G., Ghisellini G., Firmani C., Celotti A., Bosnjak Z., 2005a, *MNRAS*, 360, L45
 Ghirlanda G., Ghisellini G., Firmani C., 2005b, *MNRAS*, 361, L10
 Ghirlanda G., Nava L., Ghisellini G., Firmani C., 2007, *A&A*, 466, 127
 Golenetskii S., Aptekar R., Mazets E., Pal'shin V., Frederiks D., Ulanov, M. 2006a, *GCN Circ.*, 4989
 Golenetskii S., Aptekar R., Mazets E., Pal'shin V., Frederiks D., Cline T. 2006b, *GCN Circ.*, 5460
 Golenetskii S., Aptekar R., Mazets E., Pal'shin V., Frederiks D., Cline T. 2007a, *GCN Circ.*, 6879
 Golenetskii S., Aptekar R., Mazets E., Pal'shin V., Frederiks D., Cline T. 2007b, *GCN Circ.*, 6960
 Golenetskii S., Aptekar R., Mazets E., Pal'shin V., Frederiks D., Oleynik, P., Ulanov, M. 2007c, *GCN Circ.*, 7114
 Golenetskii S., Aptekar R., Mazets E., Pal'shin V., Frederiks D., Cline, T. 2008a, *GCN Circ.*, 7482
 Golenetskii S., Aptekar R., Mazets E., Pal'shin V., Frederiks D., Cline, T. 2008b, *GCN Circ.*, 7487
 Golenetskii S., Aptekar R., Mazets E., Pal'shin V., Frederiks D., Cline, T. 2008c, *GCN Circ.*, 7589
 Guidorzi C., 2005, *MNRAS*, 364, 163
 Guidorzi C., Frontera F., Montanari E., Rossi F., Amati L., Gomboc A., Hurley K., Mundell C. G., 2005, *MNRAS*, 363, 315

Table 2. Best-fitting parameters of the correlation between $E_{p,i}$, $L_{p,iso}$ and $T_{0:45}$.

Sample	Correlation	a	b	c	$\log(E_{p,i})$	$\chi^2 = \text{dof}$	Prob.	
all (40)	$E_{p,i} / L_{p,1s}^a T_{0:45}^b$	0.49	0.07	0.35	0.12	$1.28^{+0.19}_{-0.20}$	$0.15^{+0.05}_{-0.03}$	
all (40)	$E_{p,i} / L_{p,var}^a T_{0:45}^b$	0.46	0.07	0.35	0.13	$1.32^{+0.20}_{-0.20}$	$0.17^{+0.04}_{-0.04}$	
<i>Swift</i> (27)	$E_{p,i} / L_{p,1s}^a T_{0:45}^b$	$0.56^{+0.10}_{-0.11}$	$0.39^{+0.15}_{-0.16}$	$1.12^{+0.28}_{-0.30}$	$0.17^{+0.04}_{-0.04}$	$27.1=23$	0.25	
<i>Swift</i> (27)	$E_{p,i} / L_{p,var}^a T_{0:45}^b$	$0.52^{+0.11}_{-0.10}$	$0.38^{+0.16}_{-0.17}$	$1.16^{+0.29}_{-0.29}$	$0.18^{+0.07}_{-0.04}$	$27.5=23$	0.24	
all (40)	$E_{p,i} / L_{p,1s}^a T_{0:45}^b$	0.55	0.02	$0.50^{+0.02}_{-0.03}$	$1.03^{+0.05}_{-0.03}$	[0]	$218=37$	–
all (40)	$E_{p,i} / L_{p,var}^a T_{0:45}^b$	0.51	0.02	0.485	$1.07^{+0.05}_{-0.04}$	[0]	$260=37$	–

- Guidorzi C., Frontera F., Montanari E., Rossi F., Amati L., Gomboc A., Mundell C. G., 2006, MNRAS, 371, 843
- Halpern J. P., Mirabal N., 2006, GCN, 5982
- Hill G., Prochaska J. X., Fox D., Schaefer B., Reed M., 2005, GCN, 4255
- Jakobsson P. et al., 2006a, A&A, 460, L13
- Jakobsson P. et al., 2006b, A&A, 447, 897
- Jakobsson P., Fynbo J. P. U., Tanvir N., Rol E., 2006c, GCN, 5716
- Jakobsson P., Malesani D., Thoene C. C., Fynbo J. P. U., Hjorth J., Jaussen A. O., Andersen M. I., Vreeswijk P. M., 2007a, GCN, 6283
- Jakobsson P., Vreeswijk P. M., Hjorth J., Malesani D., Fynbo J. P. U., Thoene C. C., 2007b, GCN, 6952
- Jakobsson P., Fynbo J. P. U., Malesani D., Tanvir N. R., Milvang-Jensen B., Jaansen A. O., Vreeswijk P. M., Hjorth J., 2007c, GCN, 7117
- Jakobsson P., Vreeswijk P. M., Malesani D., Jaansen A. O., Fynbo J. P. U., Hjorth J., Tanvir N. R., 2008, GCN, 7286
- Jaansen A. O., Malesani D., Fynbo J. P. U., Sollerman J., Vreeswijk P. M., 2007a, GCN, 6010
- Jaansen A. O., Fynbo J. P. U., Andersen M. I., Vreeswijk P. M., 2007b, GCN, 6216
- Kelson D., Berger E., 2005, GCN 3101
- Kulkarni S. R. et al., 1998, Nature, 393, 35
- Kulkarni S. R. et al., 1999, Nature, 398, 389
- Le Floc'h E. et al., 2002, ApJ, 581, L81
- Ledoux C., Vreeswijk P. M., Smette A., Jaansen A., Kaufer A., 2006, GCN, 5237
- Ledoux C., Jakobsson P., Jaansen A. O., Thoene C. C., Vreeswijk P. M., Malesani D., Fynbo J. P. U., Hjorth J., 2007, GCN, 7023
- Levan A. J. et al., 2007, MNRAS, 378, 1439
- Liang E., Zhang B., 2005, ApJ, 633, 611
- Malesani D., Jakobsson P., Fynbo J. P. U., Hjorth J., Vreeswijk, P. M., 2007, GCN 6651
- Malesani D., Fynbo J. P. U., Jakobsson P., Vreeswijk, P. M., Niemi S.-M., 2008, GCN 7544
- Metzger M. R., Djorgovski S. G., Kulkarni S. R., Steidel C. C., Adelberger K. L., Frail D. A., Costa E., Frontera F., 1997, Nature, 387, 878
- Mundell C. G. et al., 2007, ApJ, 660, 489
- Nakar E., Piran T., 2005, MNRAS, 360, L73
- Norris J. P., Marani G. F., Bonnell J. T., 2000, ApJ, 534, 248
- Norris J. P., Bonnell J. T., 2006, ApJ, 643, 266
- Paciesas W. S. et al., 1999, ApJS, 122, 465
- Panaiteescu A., Mészáros P., Burrows D., Nousek J., Gehrels N., O'Brien P., Willingale R., 2006, MNRAS, 369, 2059
- Perley D. A. et al., 2008, ApJ, 672, 449
- Piranomonte S. et al., 2006, GCN, 4520
- Piro L. et al., 2002, ApJ, 577, 680
- Pizzichini G., Ferrero P., Genghini M., Gianotti F., Topinka M., 2006, Adv. Sp. Res., 38, 1338
- Price P. A., 2006, GCN, 5104
- Prochaska J. X., Thoene C. C., Malesani D., Fynbo J. P. U., Vreeswijk P. M., 2007a, GCN 6698
- Prochaska J. X., Perley D. A., Modjaz M., Bloom J. S., Poznanski D., Chen H.-W., 2007b, GCN 6864
- Prochaska J. X., Murphy M., Malec A. L., Miller K., 2008a, GCN 7388
- Quimby R., Fox D., Hoeflich P., Roman B., Wheeler J. C., 2005, GCN, 4221
- Reichart E., Lamb D. Q., Fenimore E. E., Ramirez-Ruiz E., Cline T. L., Hurley K., 2001, ApJ, 552, 57
- Rizzuto D. et al., 2007, MNRAS, 379, 619
- Rol E., Jakobsson P., Tanvir N., Levan A., 2006, GCN, 5555
- Romano P. et al., 2006, A&A, 456, 917
- Sakamoto T., Frederiks D., and Cline T., 2006, GCN, 5460
- Sakamoto T. et al., 2007, astro-ph/0707.4626
- Schaefers B. E., Deng M., Band D. L., 2001, ApJ, 563, L123
- Schaefers B. E., Collazzi A., 2007, ApJ, 656, L53
- Soderberg A. M., Berger E., Ofek E., 2005, GCN, 4186
- Still A. et al., 2006, GCN, 5226
- Thoene C. C. et al., 2006a, GCN, 5373
- Thoene C. C., Fynbo J. P. U., Jakobsson P., Vreeswijk P. M., Hjorth J., 2006b, GCN, 5812
- Thoene C. C., Perley D. A., Bloom J. S., 2007a, GCN, 6663
- Thoene C. C., Jaansen A. O., Fynbo J. P. U., Jakobsson P., Vreeswijk P.M., 2007b, GCN, 6379
- Thoene C. C., Jakobsson P., Fynbo J. P. U., Malesani D., Hjorth J., Vreeswijk P.M., 2007c, GCN, 6499
- Thoene C. C., Perley D. A., Cooke J., Bloom J. S., Chen H.-W., Barton E., 2007d, GCN, 6741
- Thoene C. C., De Cia A., Malesani D., Vreeswijk P. M., 2008a, GCN, 7587
- Thoene C. C., Malesani D., Vreeswijk P. M., Fynbo J. P. U., Jakobsson P., Ledoux C., Smette A., 2008b, GCN, 7602
- Tinney C. et al., 1998, IAU Circ., 6896
- Ulanov, M. V., Golenetskii S. V., Frederiks D. D., Mazets R. L. A. E. P., Kokomov A. A., & Palshin V. D. 2005, Nuovo Cimento C Geophysics Space Physics C, 28, 351
- Vreeswijk P. M. et al., 1999, GCN 496.
- Vreeswijk P. M., Smette A., Malesani D., Fynbo J. P. U., Milvang-Jensen B., Jakobsson P., Jaansen A. O., Ledoux C., 2008a, GCN 7444
- Vreeswijk P. M. et al., 2008b, GCN 7601
- Wiersema K., Tanvir N. R., Vreeswijk P. M., Fynbo J. P. U., Starling R., Rol E., Jakobsson P., 2008b, GCN 7517

Yonetoku D., Murakami T., Nakamura T., Yamazaki R., Inoue
A.K., Ioka K., 2004, ApJ, 609, 935

This paper has been typeset from a \TeX / \LaTeX file prepared by the
author.